Light Metals 2011 *Edited by: Stephen J. Lindsay*
TMS (The Minerals, Metals & Materials Society), 2011

CHARACTERIZATION OF A FULL-SCALE PREBAKED CARBON ANODE USING X-RAY COMPUTERIZED TOMOGRAPHY

Donald Picard[1,2], Houshang Alamdari[1,2], Donald Ziegler[3], Pierre-Olivier St-Arnaud[2], Mario Fafard[2]
[1] Department of Mining, Metallurgical and Materials Engineering, 1065 avenue de la Médecine
Laval University, Quebec, QC, G1V 0A6, Canada
[2] NSERC/Alcoa Industrial Research Chair MACE[3] and Aluminum Research Center – REGAL
Laval University, Quebec, QC, G1V 0A6, Canada
[3] Alcoa Canada Primary Metals, Aluminerie de Deschambault, 1 Boulevard des Sources,
Deschambault-Grondines, QC, G0A 1S0, Canada

Keywords: Carbon Anode, Computerized Tomography, Density

Abstract

In the conventional Hall-Héroult electrolysis process, the carbon anode is formed either by pressing or by vibro-compaction. The final properties of an anode are influenced by many parameters such as raw materials properties and manufacturing process. Presently, the aluminium producers have to deal with continuous variation of raw materials properties. To minimize the effects of the raw materials variations on the final product quality, numerical modeling of the forming process is of great interest. However, it is imperative to collect data on real anodes in order to calibrate these models. Some of the most valuable data are the density and porosity distribution of a full-scale baked anode obtained with computed tomography (CT). To test the method, three cored samples of 300 mm in diameter were taken from an industrial anode and scanned with an X-Ray tomograph. Calibration standards were also used to fit the CT scan results with the experimental data.

Introduction

In the Hall-Héroult electrolysis process, the cell is composed of various materials including steel potshell, insulators, refractory concrete, carbon lining and carbon anodes. Among them only the carbon anode could be considered as a consumable item requiring regular replacement. These anodes are consumed during electrolysis and replaced after approximately 28 days of operation. Depending on the cell technology, approximately one anode per cell is replaced each day. Hence a large number of anodes and consequently a large quantity of raw materials are required to operate a plant. The aluminium producers need to deal with continuous changing of raw materials properties resulting in a wide variation of physical properties of the pre-baked anodes.

One solution to minimize the effect of the variation of raw materials properties is to use numerical simulation methods to model the manufacturing process. The objective is to predict the anode characteristics, to control the process parameters more efficiently, and to take corrective actions before the anode is produced. To achieve this goal, a series of experimental data must be first collected in order to validate the models. In the present case, the focus will be on the apparent density distribution of prebaked anodes which can be measured either by destructive sampling [1] or by nondestructive testing (NDT) methods [2, 3]. To obtain the apparent density distribution of a full-scale prebaked anode the NDT X-Ray computerized tomography (CT) method could be used. However, previous work [2] has shown that the apparent density obtained with the CT method needs to be calibrated with standard samples. In fact, the density estimated by CT scanners may be influenced by a number of parameters such as the heterogeneity of the material [4]. The present work therefore aims at the development of a CT-based method for estimation of apparent density of anode materials. Full-scale prebaked anode core samples were used for calibration and validation of this method.

Methodology

Sample preparation

Three core samples of 292.1 mm (11.5 in) in diameter were investigated in this study. The samples were taken from a full-scale prebaked anode, produced at Alcoa Deschambault Smelter and scanned using a Somatom Sensation 64 at INRS-ETE research centre in Quebec City (Figure 1). The locations of the three core samples are illustrated in Figure 2.

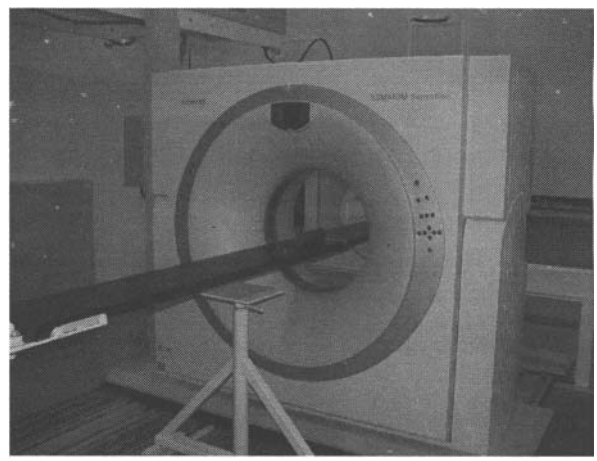

Figure 1. Somatom Sensation 64 located at the INRS-ETE (Courtesy of INRS-ETE).

In order to reveal the size effect on the CT scan results, two core samples of 152.1 mm and 50.8 mm in diameter were also taken from the same 292.1 mm samples and scanned (Figure 3). The difference in length between the samples is due the coring apparatus limitations. The upper surface of the 152.1 mm and 50.8 mm diameter samples corresponds to the bottom surface of the stub holes as shown in Figure 3. Thus, each core sample was analyzed in three different sizes. The core #3 was broken during the coring process.

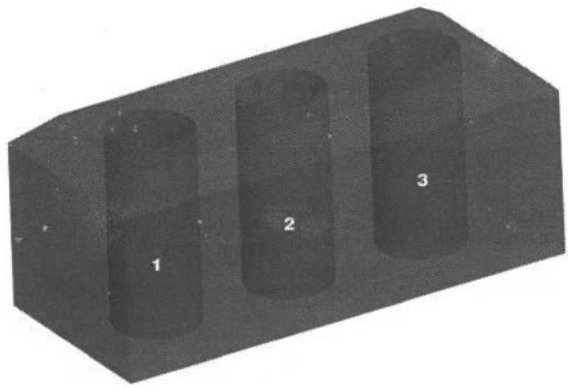

Figure 2. Anode core samples locations.

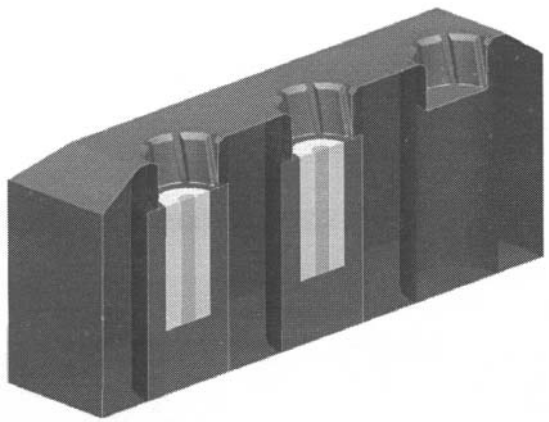

Figure 3. Location of the cores samples of different sizes. (green: ϕ 50.8 mm, yellow: ϕ 152.1 mm, red: ϕ 292.1 mm).

Anode apparent density measurement

The apparent density was measured according to the ISO 12985-1:2000(E) standard method. The samples were weighed with a precision balance (Sartorius CPA16001S) and their dimensions were measured using a CMM DEA-0101. Due to the presence of the stub holes the geometry of the 292.1 mm core samples was not regular enough to calculate its volume with high precision. Therefore, the apparent densities were measured only on the 152.1 mm and 50.8 mm samples.

X-Ray computed tomography

The X-Ray computed tomography is a method widely covered in the literature and thus will not be detailed here. In summary, this method gives the so-called *CT number* expressed in Hounsfield Units (HU) which is related to the X-Ray attenuation coefficient [2] and ranges from -1000 for air to $+3000$ for very dense materials such as metals. The density of materials with low atomic number (e.g. carbon) can be estimated by assuming a linear relation between the *CT number* and the density [5]. In that case, the calibration can be performed assuming that the density of air ($CT=-1000$) and that of water ($CT = 0$) are 0 g/cc and 1 g/cc, respectively [2]. According to this calibration, the apparent density can be calculated using the following equation:

$$\rho=0.001\times CTnumber+1 \quad (1)$$

The CT images were obtained by setting the X-Ray tube at 120 keV and 300 mA. X-Ray attenuation was measured using 0.6 mm progress steps. Each voxel (volumetric pixel) is therefore an average of the X-Ray attenuation of material with 0.6 mm of thickness. The volume of each voxel is related to the sample diameter presented in Table I.

Table I. Voxel sizes.

Core sample diameter (mm)	Volume element size (mm)
292.1	0.7×0.7×0.6
152.1	0.3×0.3×0.6
50.8	0.13×0.13×0.6

Results and discussion

X-Ray computed tomography

Only two of the three initial core samples have been analyzed (core #1 and #2). The CT scan results obtained with the core #1 are shown in Figures 4 to 6. Due to the large number of images, only some of them are shown in these figures. Each image on Figure 4 and 5 is separated by a distance of 7.8 mm while those of Figure 5 are separated by a 11.4 mm distance. Similarly, CT scan results of core #2 are shown in Figures 7 to 9. Densities are calculated based on the entire volume of the samples rather than on one image.

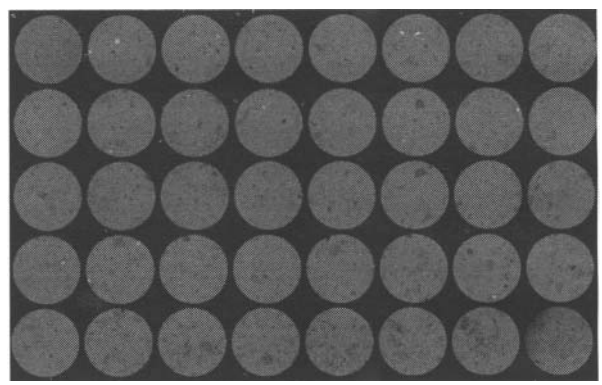

Figure 4. CT images of core #1 (ϕ 50.8 mm).

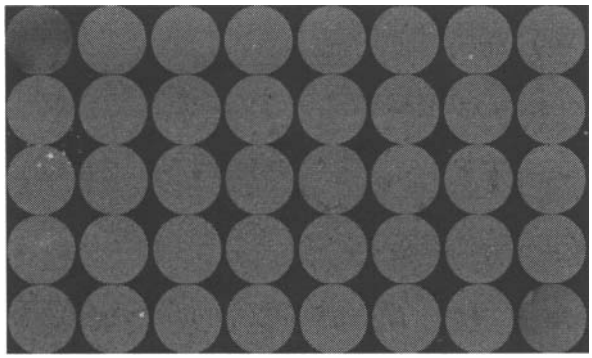

Figure 5. CT images of core #1 (ϕ 152.1 mm).

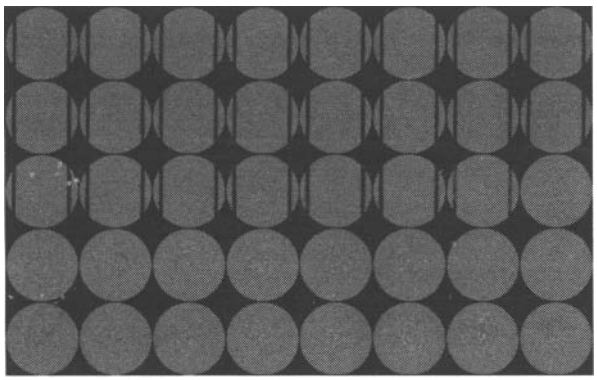

Figure 6. CT images of core #1 (ϕ 292.1 mm).

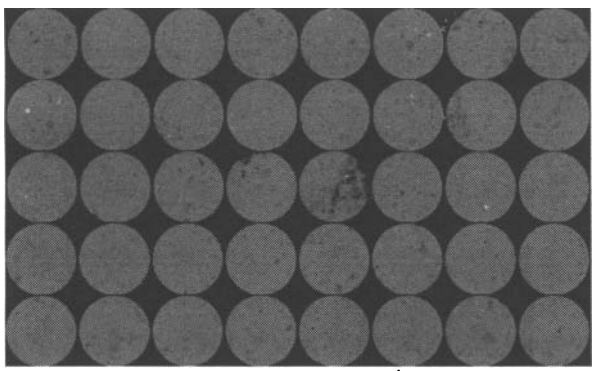

Figure 7. CT images of core #2 (ϕ 50.8 mm).

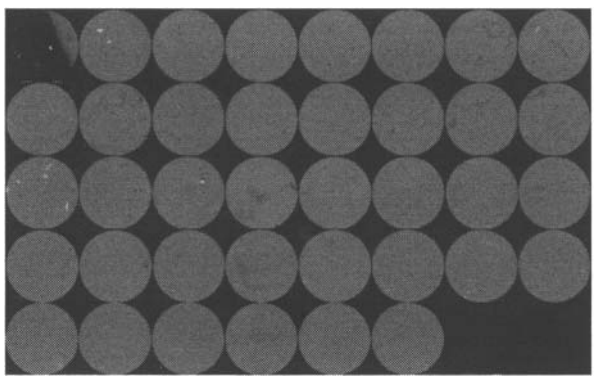

Figure 8. CT images of core #2 (ϕ 152.1 mm).

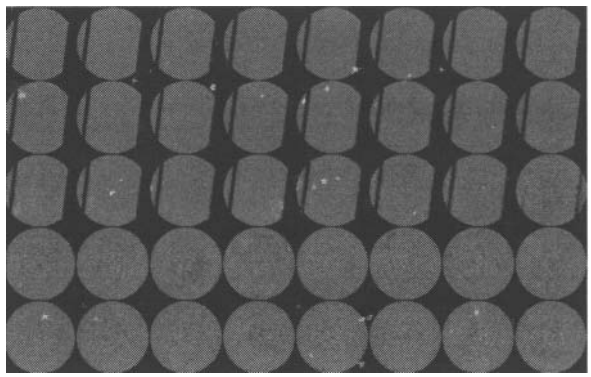

Figure 9. CT images of core #2 (ϕ 292.1 mm).

By comparing the images obtained from samples with different sizes, the effect of size on the resolution of CT scan images can clearly be seen. Aggregates and porosities are clearly visible in the small sample (Figures 4 and 7) while they are not revealed in the larger one. This is due to the fact that the voxel volume increases by increasing the sample size resulting in lower resolution. To quantify this effect the *CT number* distributions were calculated for three measurements of the core #1 and shown in Figures 10 to 12. The average values and standard deviations of *CT number* obtained for core #1 and core #2 are summarized in Tables II and III, respectively. The high standard deviations could be related to the high porosity volume fraction of material (approximately 20-25%) and to the presence of the very dense impurities with much higher *CT number* than that of carbon. These impurities are represented by the white spots on the CT images (Figures 4 to 9). The standard deviation decreases by increasing the sample size from 50.8 to 152.1 mm. This is essentially due to the increase of the voxel size. The unexpected increase in standard deviation of the *CT number* for the 292.1 mm samples is however attributed to the presence of slots in these samples. In spite of the fact that a smaller standard deviation is expected for the large samples (larger voxels), the presence of the slots introduces a large number of low density voxels, leading to increased standard deviation of the whole data set.

The average *CT number* decreases slightly (approximately 1%) by increasing the sample size suggesting that the estimated density decreases as the core size increases. Since the length of the largest diameter samples was greater than that of the smaller samples (Figure 3), the observed variation in density could also be attributed to the variation of anode density along the sample rather than only related to the sample diameter. In both cases, the density gradients within the anode and more particularly under the stub holes could explain the slight variations.

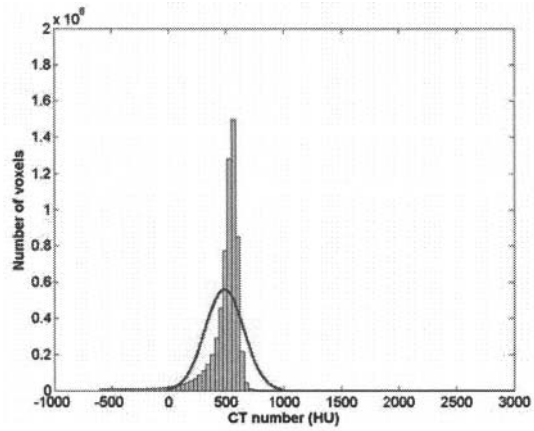

Figure 10. CT number distribution of core #1 (ϕ 50.8 mm).

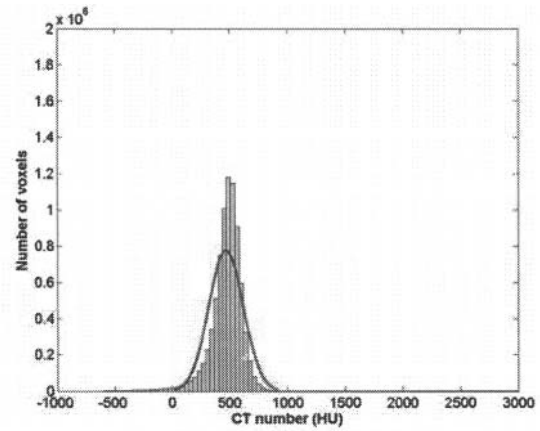

Figure 11. CT number distribution of core #1 (ϕ 152.1 mm).

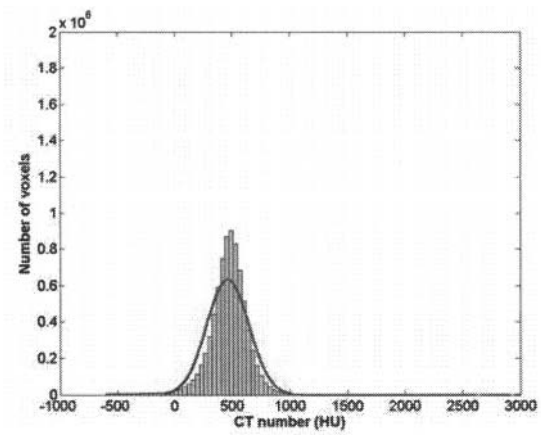

Figure 12. CT number distribution of core #1 (ϕ 292.1 mm).

Table II. Statistics of core #1.

ϕ (mm)	μ (HU)	σ (HU)
50.8	485	167
152.1	468	150
292.1	460	181

Table III. Statistics of core #2.

ϕ (mm)	μ (HU)	σ (HU)
50.8	488	167
152.1	476	149
292.1	467	168

From the *CT numbers*, the density was estimated according to equation (1) and the results were plotted in Figure 13 as a function of sample size. The estimated density was then compared to the measured apparent density as shown in Figure 14. It should be emphasized that the apparent density of the 292.1 mm samples was not measured. It can be seen that the estimated values differ significantly from the measured ones suggesting that the equation (1) does not result in accurate density estimation. The estimated apparent density is approximately 10% lower than the measured one.

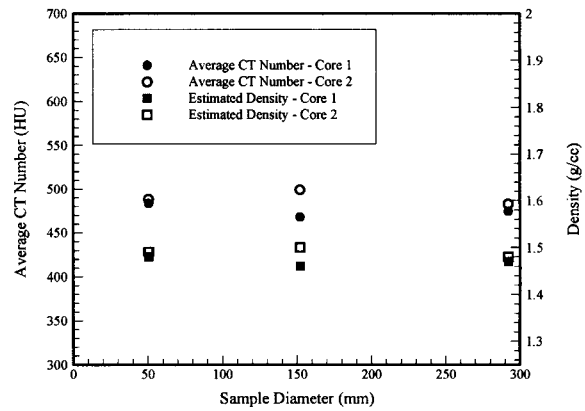

Figure 13. Estimated apparent density based on equation (1).

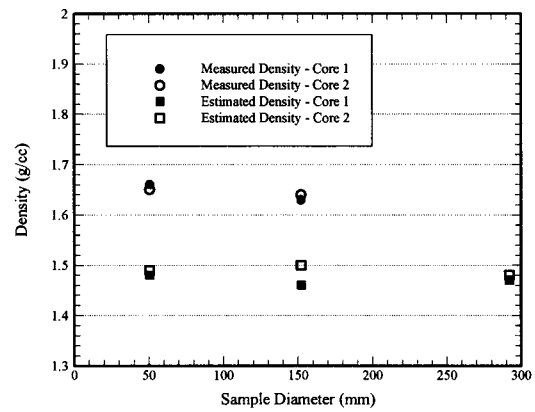

Figure 14. Comparison between the estimated and the measured apparent densities.

A new calibration was therefore performed by using the air (CT=−1000) and a representative sample instead of water. The sample of 152.1 mm diameter (taken from core #1) was used as the representative sample. Recalibration of equation (1) using air and this sample resulted in the following equation:

$$\rho = 0.0011 \times CTnumber + 1.1081 \quad (2)$$

This equation is obtained using a sample taken from the anode being studied. Therefore, one could assume that it fairly represents the effect of raw materials, fabrication process and baking procedure by which all other samples have been influenced.

The apparent density of the samples was calculated again using the equation 2. The new estimated values (called "calibrated densities") were compared with the measured densities in Figure 15. Regardless of the sample diameter, the gap between the measured density and the calibrated one has been reduced to less than 2%. This suggests that the apparent density could be accurately estimated using CT numbers when a similar material is used as calibration sample instead of water.

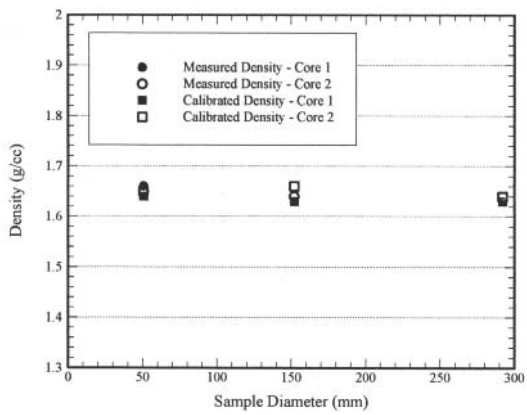

Figure 15. Comparison between the calibrated and the measured apparent densities.

The CT technique could also be used to estimate the pore volume fraction in porous materials. According to Boespflug et al. [5] the porosity of a homogeneous material could be estimated by the following relation:

$$p = \left(1 - \frac{\overline{CT} + 1024}{CT_{\max} + 1024}\right) \times 100 \quad (3)$$

Where p is the total porosity volume fraction in %, $\overline{CT}$ is the average *CT number* in HU, CT_{max} is the maximum *CT number* in HU and 1024 is the CT number of water in HU. The main issue with anode materials is to determine the CT_{max}. The prebaked anode contains not only carbon, but also other impurities with very high voxel intensity. So, only one voxel related to the impurities would be sufficient to result in an overestimated porosity percentage of the sample. In the prebaked anode studied in this work less than 1% of the voxels have intensity greater than 1000 HU. Some voxels reach however very high intensity values as great as 3000 HU. Thus, by using equation (3), a porosity volume fraction of 60% is obtained. This value is definitely inaccurate for the carbon anode. To overcome this problem one may consider limiting CT_{max} to 1000 HU, i.e. a value close to that of graphite (960 HU). The resulting porosity values with CT_{max}=1000 HU are presented in Table IV and V. The estimated porosity correlates with the measured apparent density for all samples assuming that the theoretical density of carbon is 2.21 g/cc. Typical values are however closer to 2.1 g/cc for the anode. In the later case, the porosity would be thus overestimated by equation (3) and it is thus necessary to adjust it for the anode material. This still nevertheless suggests that limiting the CT_{max} to a maximum value corresponding to that of graphite eliminates the effect of non representative voxels and results in more accurate estimations.

Table IV. Estimated total porosity of samples taken from core #1.

ϕ (mm)	μ (HU)	% voxel > 1000 HU	p (%)
50.8	485	0.03	25
152.1	468	1.43	26
292.1	460	0.63	27

Table V. Estimated total porosity of samples taken from core #2.

ϕ (mm)	μ (HU)	% voxel > 1000 HU	p (%)
50.8	488	0.03	25
152.1	476	2.76	25
292.1	467	0.63	26

Conclusion

Three samples were initially cored from a full size prebaked carbon anode in order to calibrate the relation between the X-Ray tomography intensity and the apparent density. From each main core sample, two smaller samples were cored to reveal the size effect on the average *CT numbers*. It appears that no size effect is required be taken into account.

The apparent density has been determined as a function of the *CT number*. Instead of the water, the sample of ϕ 152.1 mm of core #1 was used for calibration. The gap between the measured density and the estimated one was reduced from 10% to less than 2%. Future CT scans on different prebaked carbon anodes have to be performed to expand the validity of the new relationship within the range of anode process variations. The porosity has also been estimated using a best fit relationship. The estimated porosity tendency correlates well with the measured density of the samples.

Acknowledgements

The authors gratefully acknowledge the financial support provided by Alcoa Inc., by the Natural Sciences and Engineering Research Council of Canada and the technical support of the Aluminium Research Centre – REGAL.

References

1. Frosta, O.E., Foosnaes, T., Øye, H.A., and Linga, H., *Modelling of anode thermal cracking behaviour.* Light Metals 2008, p. 923-927.
2. Adams, A.N., Karacan, O., Grader, A., Mathews, J.P., Halleck, P.M., and Schobert, H.H., *The non-destructive 3-D characterization of pre-baked carbon anodes using X-ray computerized tomography.* Light Metals 2002, p. 535-539.
3. Suriyapraphadilok, U., Halleck, P., Grader, A., and Andresen, J.M., *Physical, chemical and X-Ray Computed Tomography characterization of anode butt cores.* Light Metals 2005, p. 617-621.
4. Duchesne, M.J., Moore, F., Long, B.F., and Labrie, J., *A rapid method for converting medical Computed Tomography scanner topogram attenuation scale to Hounsfield Unit scale and to obtain relative density values.* Engineering Geology, 2009. **103**(3-4): p. 100-105.
5. Boespflug, X., Ross, N., Long, B., and Dumais, J.F., *Axial Tomodensitometry - Relation between the Ct Intensity and the Density of the Sample.* Canadian Journal of Earth Sciences, 1994. **31**(2): p. 426-434.